



Novel Indene-[1,3,4] Oxadiazine hybrids: Design, construction, molecular docking, QSAR, ADME study and anticancer potential

Modather Farouk. Hussein^{a*}, Ibrahim O. Althobaiti^b, Hamud A. Altaleb^c,
Yasser A. A. Alossiely^a, Azzah T. Al-Enezi^a, Nadia A.A.Elkanzi^a and Rania B. Bakr^d



^aChemistry Department, College of Science, Jouf University, Sakaka 2014, Saudi Arabia

^bDepartment of Chemistry, College of Science and Arts, Jouf University, Quryat, 42421, Saudi Arabia

^cDepartment of Chemistry, Faculty of Science, Islamic University of Madinah, Madinah 42351, Saudi Arabia

^dDepartment of Pharmaceutical Organic Chemistry, Faculty of Pharmacy, Beni-Suef University, Beni-Suef 62514, Egypt

Abstract

In an attempt to improve and develop biologically potential anticancer agents, a novel set of indeno[2,1-*e*][1,3,4]oxadiazinone **2a-f** was designed and constructed *via* a reaction of ninhydrine, hydrazine hydrate and the appropriate isothiocyanate. The anticancer impact of the newly prepared compounds **2a-f** was assessed *in vitro* against A549, MCF-7 and HepG2 cell lines. The cyclohexylmethylaminoindeno[2,1-*e*][1,3,4]oxadiazinone derivative **2f** was the most active candidate towards A549 and HepG2 with IC₅₀ (64.88 and 39.18 µg/ml), respectively. A molecular docking study was done within EGFR active site to predict the binding mode of the novel compounds. Both compounds **2b** and **2f** recorded high binding energy scores with the excellent fitting with the active site. ADME study results displayed compounds **2b** and **2f** registered positive values showing good drug-likeness behaviour. Multiple linear regression analysis was used to construct consistent QSAR models based on quantum mechanics-derived chemical descriptors. Hence, it is possible to speculate that the novel compound **2f** could be considered an anticancer lead compound.

Keywords: indeno[2,1-*e*][1,3,4]oxadiazinones; anticancer; cytotoxic potential; docking study; drug-likeness.

1. Introduction

Small compounds are frequently employed in chemical biology to disrupt intricate biological processes as both therapeutic agents and research tools [1-3]. The initial plan for a mild and effective synthesis of indene derivatives focused on the base-promoted tandem Michael addition-intramolecular 5-exo cyclization reaction of starting materials. In the Michael addition procedure, several nucleophiles were employed, such as indole, imidazoles, or 2-isocyanoacetates[2].

Many pharmacological properties, including antitumor, anticoagulant, anti-inflammatory,

neuroprotective, and antibacterial, are present in indan-1,3-dione derivatives [4]. In addition, molecules with the indan-1,3-dione core have been identified from the natural world [5,6]. For instance, the natural spiro indan-1,3-dione fredericamycin A exhibits antitumor antibiotic action [7,8]. Indane-1,3-dione and its derivatives play important roles in biological processes and are essential in synthesizing chemical molecules. Numerous compounds of leishmanicidal and cytotoxic 2-arylidene indane 1,3-diones [9].

*Corresponding author e-mail: mfhussin@ju.edu.sa (Modather Farouk. Hussein)

Received date 13 June 2023; revised date 28 July 2023; accepted date 10 August 2023

DOI: 10.21608/EJCHEM.2023.216875.8133

©2024 National Information and Documentation Center (NIDOC)

Indanone derivatives have received a great deal of attention since many synthetically bioactive compounds incorporating the indanone scaffold were reported to reveal a wide range of biological potential as anti-inflammatory [10-12], antimicrobial [13-15], antioxidant [16], monoamine oxidase inhibitors [17,18], antiviral [19-22] and anticancer [23-28]. Novel indanones were constructed and assessed for their anticancer potential against breast carcinoma cell line MCF-7 and cervical carcinoma cell line (HELA) [29]. Oxadiazine heterocycle drawn chemists' attention due to its potential pharmacological activities as an antioxidant [30,31], anti-hepatotoxic [32], insecticide [33,34], antimicrobial [35,36], monoamine oxidase inhibitor [37], anticancer [38-40]. New derivatives of oxadiazines had been synthesized and screened for their anticancer activity against breast adenocarcinoma (MCF-7), CNS cancer (SF-268) and non-small cell lung cancer (NCI-H460) [41].

One of the most significant classes of insecticides was the oxadiazine pesticides. The DuPont Company created the revolutionary broad-spectrum oxadiazine insecticide Indoxacarb, which was a well-known inhibitor of sodium channels and has shown exceptional field activity, high efficiency, mammalian safety, low toxicity, environmental compatibility, no cross-resistance, and a novel method of action with great crop protection and minimal mammalian toxicity [42-44].

Continuing our efforts to construct novel heterocycles with potent pharmacological potential [45-54], we record here a modification of indanone into condensed Oxadiazine derivatives incorporating the indanone moiety. The molecular mechanisms of anticancer drug interactions are currently poorly understood. This tremendously complex subject would benefit greatly from the alternative, the more adaptable viewpoint that computational tools like Quantitative Structure-Activity Relationship (QSAR) can provide. A credible predictive QSAR model may provide fresh insights into the medications' action mode while guiding molecular screening and design [55-57]. The underlying premise of all QSAR research is that structurally related compounds have similar physicochemical properties and are expected to have a similar biological effect. In general, molecular features such as electronic, hydrophobic, steric, hydrogen bonding, and dispersion properties may all be useful in characterizing the many working processes of drug action [58,59]. In certain circumstances, all molecular descriptors are crucial, but in others, just a handful are, and the remainders play only a minor role. [60]. This is true in the current work, as we discovered that electronic characteristics, specifically frontier-orbital energies

and hydrophobicity, can effectively correlate pharmacological activity.

Cancer is a rapidly mutated disease. There are more than a hundred different varieties of cancer, each with a unique behaviour and response to therapy [61]. The abnormal multiplication of any cell may cause cancer. Cancer recurrence in the same organ or other organs occurs in a process called metastasis even after surgery or radiotherapy [62]. The advancement of cancer biology research and the advent of new paradigms in the study of metastasis have helped shed light on some of the molecular underpinnings of this spreading process. Due to the escalating prevalence of cancer, additional research and the development of new treatments are required. Cancer treatment resistance develops upon cell mutation, genetic variations and even radiation [63]. Patients suffering from more than one type of cancer simultaneously are in despite need of systemic medications to control all the types, so a strategy involved synthesis of new multitarget anticancer compounds is critical.

Quantitative structure-activity relationship (QSAR) models are frequently used to search sizable databases of chemicals and identify the biological characteristics of chemical molecules based on their chemical structure. As time goes on, the data on known and synthesized chemicals will continue to rise exponentially, necessitating automated QSAR modeling methods that are computationally efficient and accessible to academics that may not have a deep understanding of machine learning modeling. So, the QSAR community may benefit from having a completely automated and sophisticated modeling platform [64].

The goal of QSAR modeling is to discover the relationship between anticancer activity and molecular structure. A multi-linear equation that relates molecular structural features to the desired activity is most often used to express the relationship [65].

$$\text{Activity} = \sum_i x^i a^i + b$$

Where x stands for the molecular descriptor and a are the parameters to be optimized using a known data set, and b is constant.

Two processes must occur when a chemical molecule is delivered to an organism to elicit a biological reaction. First, the substance must be delivered to the site of action (receptor), and then it must interact appropriately with the target.

The molecular descriptors are numerical representation of molecules that describe the interaction effects of molecules such as Homo, Lumo, ionization potential, dipole moments, or drug

delivery and size effects such as hydrophobic/hydrophilic solvent-surface areas, octanol-water partition coefficient, solvation energy power, and molecular weight. After that, all descriptors were considered potential predictor variables in multiple linear regressions for the outcome measure log (IC₅₀).

In the current study, we aim to synthesize new heterocycle indenooxadiazinones and evaluate their in vitro anticancer potentials towards three cell lines; breast cancer cell line (MCF-7), lung cancer cell line (A549) and liver cancer cell line (HepG2). In addition, molecular modeling studies were carried out to predict the mode of action of the novel indenooxadiazinone derivatives. Molecular docking and QSAR study were performed on the new synthetic compounds as a tool of computational drug design to discover novel anticancer agents.

2. Results and discussion

2.1. Chemistry

Synthesis of novel indenooxadiazinones **2a-f** was established. The synthetic route for the construction of 4a-hydroxy-3-mercapto-3-(substitutedamino)-2,3-dihydroindeno[2,1-*e*][1,3,4]oxadiazin-9(4a*H*)-ones **2a-f** was outlined in Scheme 1. The reaction of ninhydrin, hydrazine hydrate and the appropriate isothiocyanate in methanol under reflux for 6-7 hr. produced the target compounds **2a-f** in high yield. The proposed mechanism for forming the indenooxadiazinones **2a-f** is explained (Figure 1).

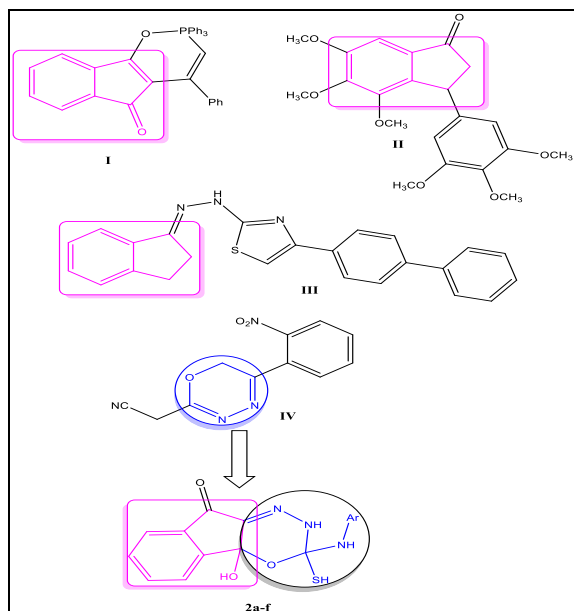
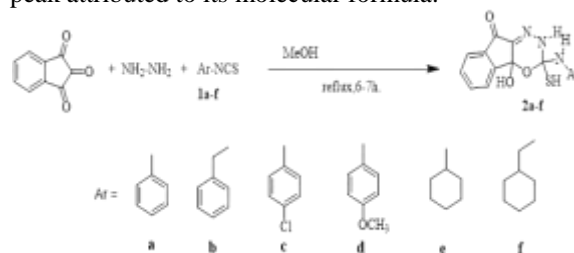


Fig. 1: Chemical structures of indanones **I-III**, oxadiazines **IV** and the novel candidates **2a-f** with anticancer activity. The chemical structures of indenooxadiazinones **2a-f** were elucidated by elemental and spectral tools. IR spectra disclosed the appearance of stretching bands

at 2745-2740, 3122-3125 and 3425-3421 cm⁻¹ which attributed to SH, NH and OH, respectively. In addition, the existence of five singlet signals at 3.65, 7.36, 8.5, 9.02 and 10.20 ppm attributed to CH₂, SH, 2NH and OH protons in the chart of ¹HNMR of compound **2f** proved the structure. Moreover, the appearance of methoxy protons of **2d** at 3.46 ppm also confirmed the structure (Figures S1-S6). Each compound's mass spectrum displayed a molecular ion peak attributed to its molecular formula.



Scheme 1: Construction of compound **2a-f**.

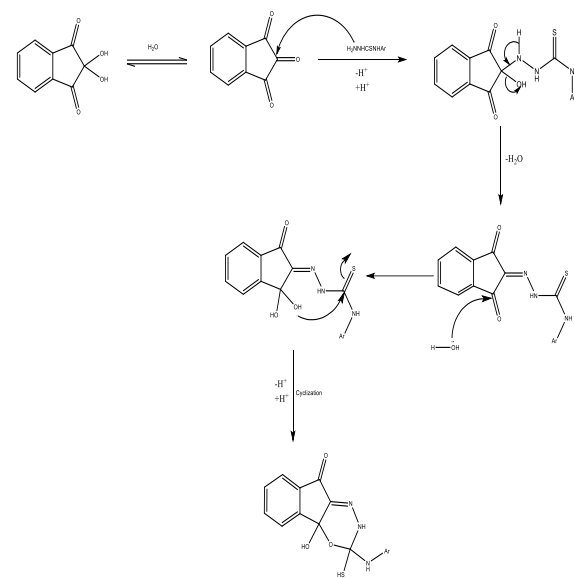


Fig. 2: Proposed mechanism for the formation of the target compounds **2a-f**

2.2. Anticancer potential

The cytotoxic potential of the newly constructed indeno[2,1-*e*][1,3,4]oxadiazin-9-one was estimated against three human cancer cell lines, including breast cancer cell line (MCF-7), lung cancer cell line (A549) and liver cancer cell line (HepG2) applying MTT assay in comparison to doxorubicin as a standard. The parameter IC₅₀ represents the concentration required to inhibit cell viability by 50% (Figure 3). Towards the three tested cell lines, MCF-7, A549 and HepG2, the

benzylaminoindenoaxadiazinone derivative (**2b**) ($IC_{50} = 95.02, 99.57$ and $110 \mu\text{g/ml}$, respectively) and cyclohexylmethylaminoindenoaxadiazinone derivative (**2f**) ($IC_{50} = 87.11, 64.88$ and $39.18 \mu\text{g/ml}$, respectively) exhibited high efficacies compared to doxorubicin ($IC_{50} = 70, 50.47$ and $67.59 \mu\text{g/ml}$, respectively). On the other hand, other indenoaxadiazinone derivatives **2a**, **2c**, **2d** and **2e** revealed weak anticancer potential with IC_{50} of 419.0, 227.87, 307.01, 317.22 $\mu\text{g/ml}$, sequentially against MCF-7, IC_{50} of 164.46, 129.93, 134.01, 222.2 $\mu\text{g/ml}$ towards A549 and IC_{50} of 217.82, 165.92, 154.83, 211.36 towards HepG2. Furthermore, the cyclohexylmethylamino derivative (**2f**) depicted comparable anticancer activity towards MCF7 ($IC_{50} = 87.11 \mu\text{g/ml}$) and A549 ($IC_{50} = 64.88 \mu\text{g/ml}$) to that exhibited by doxorubicin ($IC_{50} = 70$ and $50.47 \mu\text{g/ml}$, respectively). Finally, compound **2f** was more potent against hepatic cancer cell line (HepG2) ($IC_{50} = 39.18 \mu\text{g/ml}$) than the standard drug doxorubicin ($IC_{50} = 67.59 \mu\text{g/ml}$). These results show the high anticancer effect of **2f** on A549 and HepG2 cell lines.

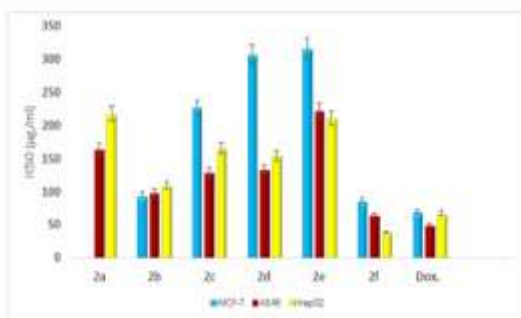


Figure 3: *In vitro* cytotoxicity for indenoaxadiazole derivatives **2a-2f** and doxorubicin (Dox.) against MCF-7, A549 and HepG2 cell lines

2.3. Docking study

Epidermal growth factor receptor (EGFR) is a transmembrane growth factor protein tyrosine kinase [54,66]. EGFR significantly impacts signal transduction and cell survival [67]. Figure 4: Binding energy score (kcal/mol) for all constructed compounds **2a-f** and erlotinib. To predict the mechanism of the anticancer potential of the newly constructed candidates **2a-f**, a docking study was conducted into ATP binding region of EGFR. The X-ray crystal of EGFR with the cocrystallized ligand erlotinib was obtained from a protein data bank (PDB: 1M17). Erlotinib was redocked to validate the docking protocol utilizing the MMFF94 force field. The binding energy for the newly constructed compounds (**2a-f**) docked within EGFR active region shows the best compounds obtained in docking analyses (Figure 4).

The larger the peak, the lower binding energy and so better binding within the active site with predictable

higher anticancer potential.

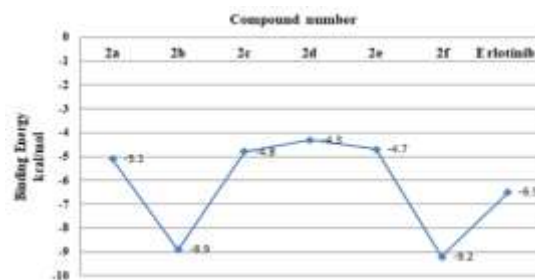


Figure 4: Binding energy score (kcal/mol) for all constructed compounds **2a-f** and erlotinib.

The docking outcomes, including binding energy ΔG and types of interaction, are listed (Table 1). The benzylaminoindeno[2,1-*e*][1,3,4]oxadiazinone (**2b**) ($\Delta G = -8.9$ kcal/mol) and cyclohexylmethylaminoindeno [2,1-*e*][1,3,4]oxadiazinone derivatives (**2f**) ($\Delta G = -9.2$ kcal/mol) recorded higher binding energy than registered by the cocrystallized ligand erlotinib (-6.5 kcal/mol). The cyclohexylmethylamino derivative formed three H-bonds within the active region with GLU738 and LYS721 *via* binding with SH and OH groups, in addition to the formation of alkyl binding with ALA731 (Figure 5).

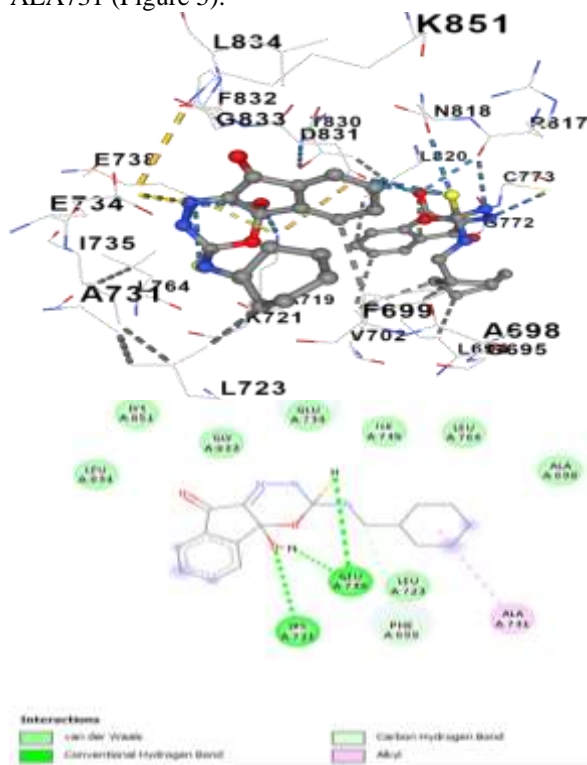


Figure 5: The suggested binding mode of compound **2f** within the binding region of EGFR A) 3D form B) 2D form.

The benzylamino derivative **2b** displayed excellent fitting within the active site forming several types of binding: I) Hydrogen bonds with ASP831 and THR830, II) Pi-Alkyl binding with LYS721,

ALA719 and LEU764, III) Pi-donor Hydrogen bond with THR766, IV) Pi-anion binding with ASP831 and V) Pi-Pi stacked interaction with PHE699 (Figure 6).

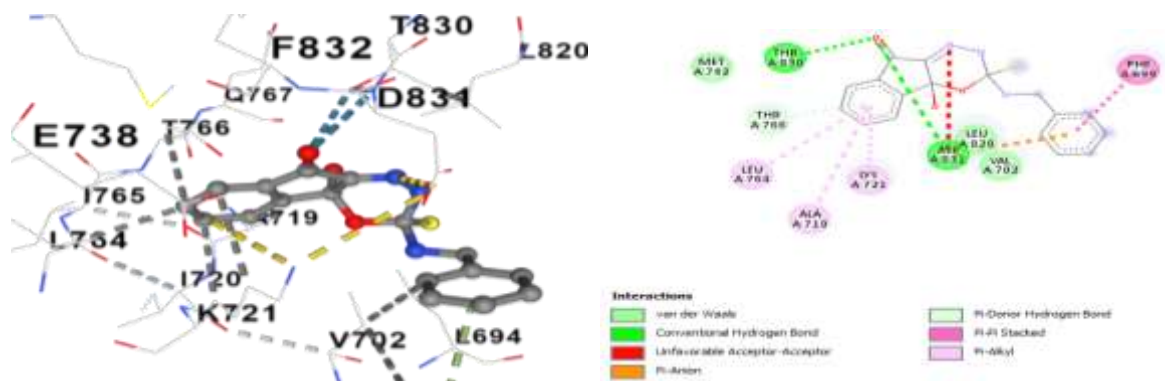


Figure 6: The suggested binding mode of compound **2b** within the binding region of EGFR A) 3D form B) 2D form.

Table 1.

Docking outcomes of the newly constructed dihydroindeno[2,1-*e*][1,3,4]oxadiazin-9(4*aH*)-one derivatives (**2a-f**)

NO.	Docking score Kcal/mol	No. of bonds	Type of interactions	Amino acids	Function group
2a	-5.1	2	H-bond Pi-Pi staked	ASP831 PHE699	NH Phenyl moiety
2b	-8.9	4	H-bond H-bond H-bond Alkyl binding	GLU738 GLU738 LYS721 ALA731	OH SH OH Cyclohexyl
2c	-4.8	1	H-bond	GLU738	OH
2d	-4.3	1	Pi-alkyl	ALA674	Phenyl
2e	-4.7	2	Pi-alkyl	ALA719 LYS721	Phenyl ring Phenyl ring
2f	-9.2	8	H-bond H-bond Pi-donor H bond Pi-alkyl Pi-alkyl Pi-alkyl Pi-anion Pi-Pi stacked	Thr830 Asp831 Thr766 LYS721 ALA719 Leu764 Asp831 PHE699	C=O C=O Phenyl ring Phenyl ring Phenyl ring Phenyl ring Phenyl ring Benzyl ring Benzyl ring
Doxo.	-6.5	2	H-bond H-bond	MET769 LYS721	OCH ₃ Quinazoline N-3

2.4. ADME study and drug-likeness

Lipinski rule was utilized to predict the biochemical properties of the novel candidates 2a-f. This rule states that an orally potential drug has no more than 5 HBD, no more than 10 HBA, Log_p should be less

than 5, and molecular mass should be less than 500 g/mol. All compounds' molecular mass was within the range (327.37-361.81 g/mol). All compounds scored 3 HBD and 6-7 HBA regarding HBD and HBA. Log_p for all the constructed candidates

fulfilled the standard value (< 5). Moreover, topological surface area (TPSA) ranged from 82.15-92.19 Å^2 which justified the standard value ($< 140 \text{Å}^2$) (Figure 7 & Table 2).

Drug-likeness describes many molecular properties such as hydrophobicity, electronic distribution, and molecular size, and hydrophobicity. The results displayed good scores, especially compounds 2b and 2f registered positive values showing good drug-likeness behavior.

2.5. QSAR Module

QSAR was made for several previously published indene derivatives listed in table 3 [70,71], with IC50 values. To calculate the QSAR, firstly, calculation of the molecular descriptors for all compounds then fits these compounds with a new synthesized indene compounds to calculate the predicted IC50 according to the following multiple linear regression equation:

$$\text{-Log IC50} = -2.517 - 0.036 \text{ dipole moment} - 0.038 E_{\text{Homo}} + 0.022 E_{\text{Lumo}} + 0.001 \text{ ASA} + 0.135 \text{ Acc} - 0.289 \text{ don} + 0.017 \text{ Esol} - 0.113 \log P(\text{o/w}) + 0.003 \text{ Weight}$$

Table 4 and Figure 8 correlate the expected and actual IC50 values. The theoretical and empirical values show a strong connection and convergence, suggesting that this method can be used to forecast anticancer efficacy. However, compound 2f is closer to the harmony between the theoretical value estimated from QSAR and laboratory values from attached cancer cells. There is a considerable variation in the values of the compounds prepared from 2a -f. QSAR studies have generally demonstrated their ability to forecast the effectiveness of medicinal organic molecules against cancer

Table 2. Predicted Lipinski parameters for the newly constructed compounds **2a-f**

Candidate number	M. wt.	HBD	HBA	CLogP	TPSA	n violation	Rotatable bonds	DLS
2a	327.37	3	6	2.02	82.95	0	2	-0.64
2b	341.39	3	6	1.72	82.95	0	3	0.11
2c	361.81	3	6	2.70	82.95	0	2	0.06
2d	357.39	3	7	2.08	92.19	0	3	-0.33
2e	333.41	3	6	2.23	82.95	0	2	-0.15
2f	347.44	3	6	2.61	82.95	0	3	0.59

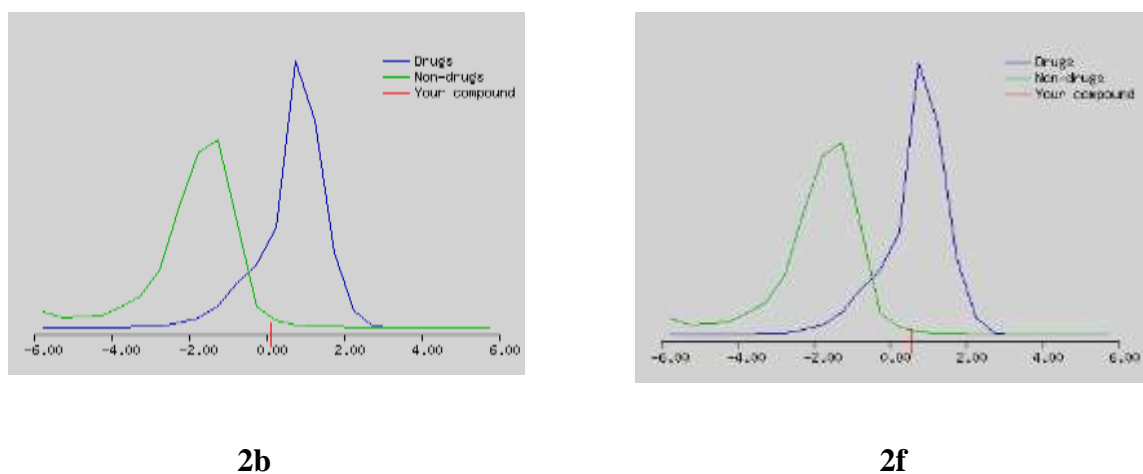
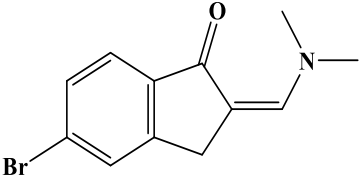
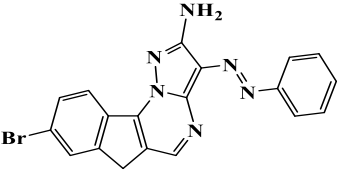
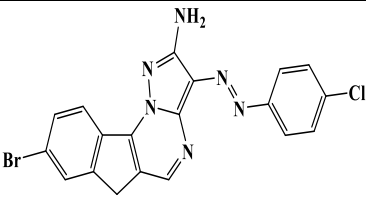
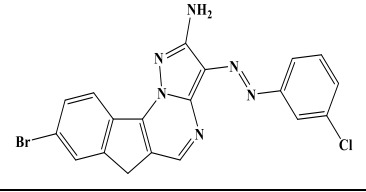
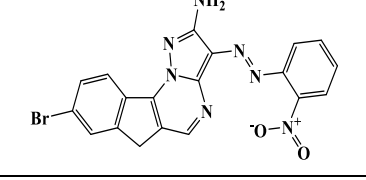
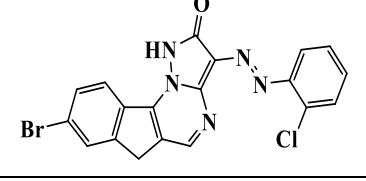
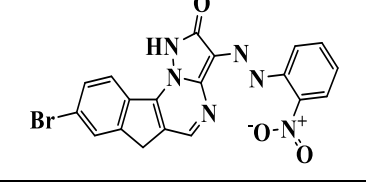

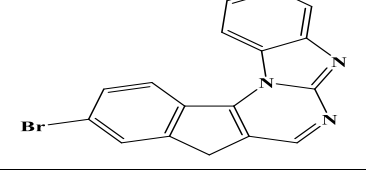
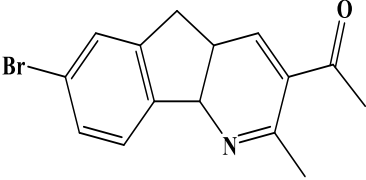
Fig.7. Drug likeness of compounds **2b** and **2f**

Table 3: QSAR descriptors for some indene derivatives

Molecules	IC50	-logIC50	AM1_ dipole	AaM1_ HOMO	AM1_ IP	AM1_ LUMO	ASA	a_ac c	a_don	E_sol	logP(o/ w)	Weight
	100	-2	1.3535	-8.852	8.8519	-1.1767	494.83	1	0	-14.68	2.393	266.13
	27	-1.431	2.2372	-8.205	8.2054	-1.3085	614.48	4	1	-15.31	4.788	405.25

Molecules	IC50	-logIC50	AM1_dipole	AaM1_HOMO	AM1_IP	AM1_LUMO	ASA	a_acc	a_don	E_sol	logP(o/w)	Weight
	37	-1.568	6.8462	-7.840	7.8406	-1.5534	773.95	4	1	-28.92	5.38	439.70
	40	-1.602	2.1116	-8.351	8.3512	-1.3368	754.30	4	1	-33.14	5.417	439.70
	100	-2	4.9332	-9.247	9.2472	-1.2341	711.40	4	1	-42.01	4.721	450.25
	38	-1.579	2.5256	-8.987	8.9871	-1.4273	756.82	4	1	-27.97	5.848	440.68
	100	-2	5.1808	-9.883	9.8836	-2.9039	723.43	4	1	-40.70	5.191	451.24
	62	-1.792	3.6007	-9.359	9.3591	-1.837	516.99	3	0	-21.68	1.904	287.12
	76	-1.880	4.3785	-8.569	8.5699	-1.4037	486.46	2	0	-11.35	4.81	336.19
	33	-1.518	3.6287	-9.388	9.3881	-0.2571	548.21	2	0	-11.48	2.508	304.18

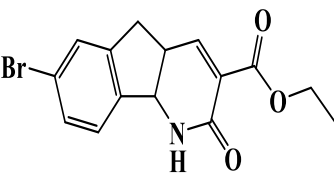
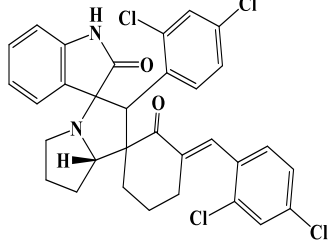
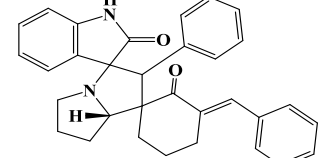
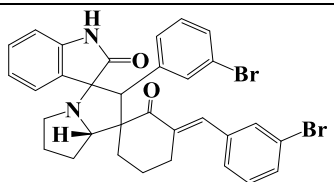
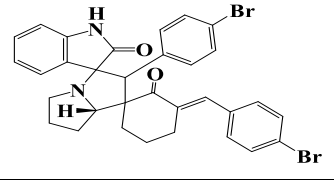
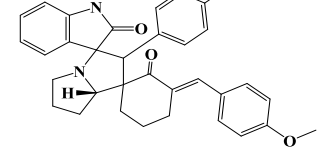
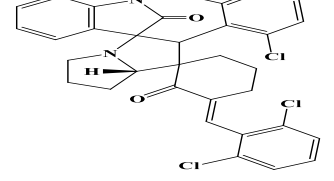
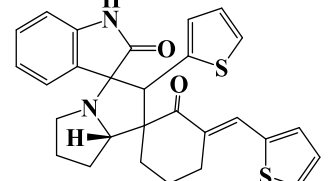
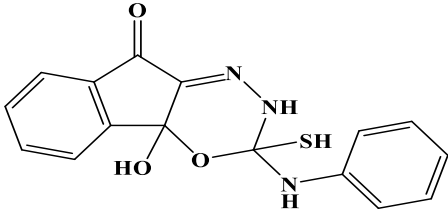
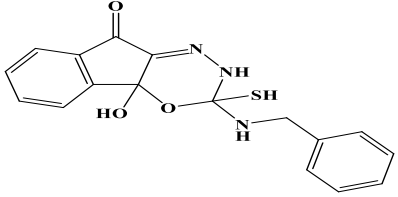
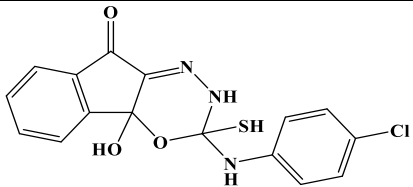
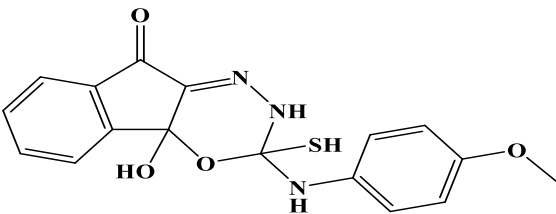
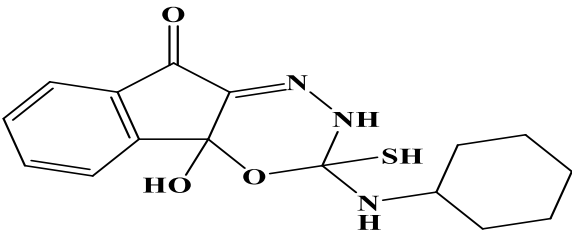
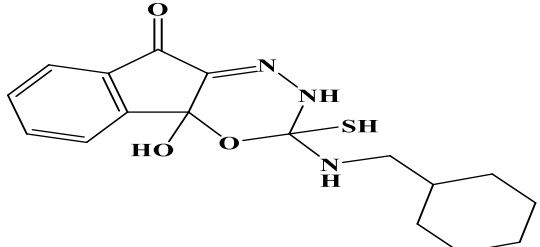
Molecules	IC50	-logIC50	AM1_ dipole	AaM1_ HOMO	AM1_ IP	AM1_ LUMO	ASA	a_ac c	a_don	E_sol	logP(o/ w)	Weight
	100	-2	3.5706	-9.683	9.6834	-0.5814	548.01	2	1	-18.87	2.332	336.18
	22	-1.342	5.5205	-8.834	8.8341	-0.7676	886.26	3	1	-27.17	7.738	612.38
	39	-1.591	1.0037	-8.880	8.8807	-0.1853	718.04	3	1	-16.73	5.3	474.60
	20	-1.301	3.6979	-8.576	8.5768	-0.6804	763.55	3	1	-23.90	6.97	632.39
	19	-1.278	9.3126	-8.553	8.5535	-1.0402	911.00	3	1	-31.55	6.896	632.39
	30	-1.477	27.252	-4.502	4.5026	-3.151	998.97	5	1	-14.35	5.212	534.65
	43	-1.633	8.5574	-6.207	6.2076	-3.8692	886.28	3	1	-37.30	7.66	612.38
	24	-1.380	7.2249	-8.299	8.2997	-1.6297	708.61	3	1	-27.02	4.36	486.66

Table 4: Correlation between actual and predicted IC50 of the Synthesized molecules

n	Molecule	Predicted	-Log IC50 Actually		
		-Log IC50	Mcf-7	A549	HepG2
2a		-1.94266	-2.62256	-2.21606	-2.3381
2b		-1.90867	-1.97772	-1.99813	-2.04395
2c		-1.85891	-2.35769	-2.11371	-2.2199
2d		-1.88621	-2.48824	-2.12714	-2.18986
2e		-1.92597	-2.50136	-2.34688	-2.32502
2f		-1.89829	-1.94007	-1.81211	-1.59306

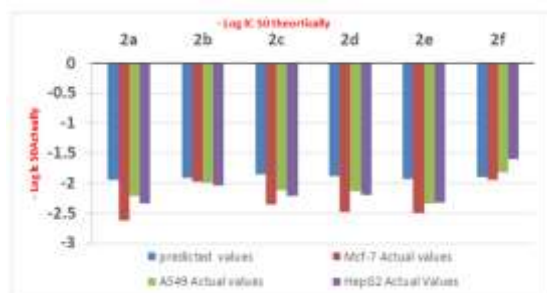


Figure 8: Relationship between synthesized compounds' actual and predicted -log IC₅₀.

3. Experimental

3.1. Chemistry

All solvents and reagents are purchased from Sigma-Aldrich and used without purification. Thin-layer chromatography (TLC) on silica gel pre-coated F254 Merck plates was utilized to monitor the reaction progress. Melting points of all constructed compounds were measured without correction utilizing Gallenkam electrothermal (Weiss Gallenkam, Loughborough, UK). Infrared spectra were obtained on a Perkin Elmer Lambda 40 spectrometer using KBr pellets. Nuclear magnetic resonance (¹H-NMR and ¹³C-NMR) were recorded on Varian VXR300/5 FT NMR spectrometer at 300 MHz in DMSO-*d*₆. Electron ionization mass spectrometry (EIMS) was done with the use of Finnegan Trace Gas Chromatography Polaris Q-spectrometer. Elemental analysis was measured by PerkinElmer elemental analyzer at Micro analytical Center, Cairo University.

General synthetic procedure for 2a-f: A mixture of 2 mmol of hydrazine hydrate, 2 mmol isothiocyanate derivatives, and 2 mmol of ninhydrin in 10 mL of MeOH was heated under reflux at 6-7 hours monitored by TLC, the solvent was evaporated and the precipitate collected and recrystallized from ethanol

4a-Hydroxy-3-mercapto-3-(phenylamino)-2,3-dihydroindeno[2,1-*e*][1,3,4]oxadiazin-9(4aH)-one (2a)

(80% yield) as green solid, mp 216-218°C, IR (KBr): ν (cm⁻¹) 1649 (C=O), 3223-3339 (2NH & OH); ¹H NMR (DMSO-*d*₆): δ 7.22- 7.64 (m, 9H, Aromatic proton), 9.46 (s, 1H, NH), 9.72 (s, 1H, NH), 9.81 (s, 1H, OH), 11.27 (s, 1H, SH); ¹³C NMR (DMSO-*d*₆): 88.17, 130.80, 131.13, 131.39, 132.47, 132.98, 137.75, 142.49, 144.25, 145.82, 172.10; ms (m/z, %): 327.0 (M⁺, 50%). Anal. Calcd for C₁₆H₁₃N₃O₃S (327.36): C, 58.70; H, 4.00; N, 12.84; S, 9.80%. Found: C, 58.75; H, 4.09; N, 12.88; S, 9.86.

3-(Benzylamino)-4a-hydroxy-3-mercapto-2,3-dihydroindeno[2,1-*e*][1,3,4]oxadiazin-9(4aH)-one (2b)

(75% yield) as Orange solid, mp 233-235°C, IR (KBr): ν (cm⁻¹) 1723 (C=O), 3115-3340 (2NH & OH); ¹H NMR (DMSO-*d*₆): δ 4.10 (s, 2H, CH₂), 7.65- 7.86 (m, 9H, Aromatic proton), 10.18 (s, 1H, NH), 10.27 (s, 1H, NH), 10.34 (s, 1H, OH), 12.68 (s, 1H, SH); ¹³C NMR (DMSO-*d*₆): 51.18, 117.49, 121.44, 123.94, 128.69, 129.89, 131.22, 131.67, 145.83, 153.53, 193.00; ms (m/z, %): 341.0 (M⁺, 45%). Anal. Calcd for C₁₇H₁₅N₃O₃S (341.38): C, 59.81; H, 4.43; N, 12.31; S, 9.39%. Found: C, 59.86; H, 4.47; N, 12.36; S, 9.42.

3-((4-Chlorophenyl)amino)-4a-hydroxy-3-mercapto-2,3-dihydroindeno[2,1-*e*][1,3,4]oxadiazin-9(4aH)-one (2c)

(74% yield) as yellow solid, mp 245-247°C, IR (KBr): ν (cm⁻¹) 1667 (C=O), 3127-3313 (2NH & OH); ¹H NMR (DMSO-*d*₆): δ 7.61- 7.98 (m, 8H, Aromatic proton), 9.80 (s, 1H, NH), 10.45 (s, 1H, NH), 10.50 (s, 1H, OH), 12.00 (s, 1H, SH); ¹³C NMR (DMSO-*d*₆): 130.57, 130.95, 131.05, 131.84, 135.37, 142.10, 143.16, 144.30, 147.10, 187.31; ms (m/z, %): 361.0 (M⁺, 45%). Anal. Calcd for C₁₆H₁₂ClN₃O₃S (361.80): C, 53.11; H, 3.34; Cl, 9.80; N, 11.61; S, 8.86%. Found: C, 53.15; H, 3.36; Cl, 9.85; N, 11.66; S, 8.89.

4a-Hydroxy-3-mercapto-3-((4-methoxyphenyl)amino)-2,3-dihydroindeno[2,1-*e*][1,3,4]oxadiazin-9(4aH)-one (2d)

(80% yield) as red solid, mp 226-228°C, IR (KBr): ν (cm⁻¹) 1668 (C=O), 3122-3319 (2NH & OH); ¹H NMR (DMSO-*d*₆): δ 3.78 (s, 3H, CH₃), 7.44- 8.21 (m, 8H, Aromatic proton), 10.19 (s, 1H, NH), 11.01 (s, 1H, NH), 12.74 (s, 1H, OH), 13.31 (s, 1H, SH). ¹³C NMR (DMSO-*d*₆): 63.38, 128.73, 129.38, 130.75, 130.93, 131.06, 131.84, 134.28, 143.16, 150.81, 188.96; ms (m/z, %): 357.0 (M⁺, 30%). Anal. Calcd for C₁₇H₁₅N₃O₄S (357.38): C, 57.13; H, 4.23; N, 11.76; S, 8.97%. Found: C, 57.17; H, 4.26; N, 11.78; S, 8.99.

3-(Cyclohexylamino)-4a-hydroxy-3-mercapto-2,3-dihydroindeno[2,1-*e*][1,3,4]oxadiazin-9(4aH)-one (2e)

(68% yield) as reddish brown solid, mp 252-254°C, IR (KBr): ν (cm⁻¹) 1690 (C=O), 3194-3452 (2NH & OH); ¹H NMR (DMSO-*d*₆): 1.07 (t, 2H, CH₂), 1.91 (m, 2H, CH₂), 3.29 (s, 1H, CH), 7.24-7.40 (m, 4H, Aromatic proton), 10.25 (s, 1H, NH), 10.54 (s, 1H, NH), 12.06 (s, 1H, OH), 12.18 (s, 1H, SH); ¹³C NMR (DMSO-*d*₆): 23.36 (CH₂), 24.43 (CH₂), 25.61 (CH₂), 115.54 (CH), 97.41 (C-OH), 123.13, 124.14, 125.26, 127.27, 129.09, 131.09, 133.29, 137.38 (ArC), 150.65 (C=N), 185.56 (C=O); ms (m/z, %): 333.0 (M⁺, 30%). Anal. Calcd for C₁₆H₁₉N₃O₃S (333.41): C, 57.64; H, 5.74; N, 12.60; S, 9.62%. Found: C, 57.67; H, 5.79; N, 12.64; S, 9.65.

3-((Cyclohexylmethyl) amino)-4a-hydroxy-3-mercapto-2,3-dihydroindeno[2,1-e][1,3,4]oxadiazin-9(4aH)-one (2f)

(65% yield) as pale yellow solid, mp 238-240°C, IR (KBr): ν (cm⁻¹) 1719 (C=O), 3179-3435 (2NH & OH); ¹H NMR (DMSO-d₆): 1.07 (t, 2H, CH₂), 2.45 (m, 2H, CH₂), 3.45 (s, 2H, CH₂), 4.30 (s, 1H, CH), 7.46-7.93 (m, 4H, Aromatic proton), 10.19 (s, 1H, NH), 10.27 (s, 1H, NH), 11.33 (s, 1H, OH), 12.78 (s, 1H, SH); ¹³C NMR (DMSO-d₆): 23.36 (CH₂), 24.43 (CH₂), 25.61 (CH₂), 43.02(CH₂), 115.54 (CH), 97.41(C-OH), 123.13, 124.14, 125.26, 127.27, 129.09, 131.09, 133.29, 137.38(ArC), 150.65 (C=N), 185.56 (C=O); ms (m/z, %): 347.0 (M+, 25%). Anal. Calcd for C₁₇H₂₁N₃O₃S (347.43): C, 58.77; H, 6.09; N, 12.09; S, 9.23%. Found: C, 58.79; H, 6.17; N, 12.15; S, 9.28.

3.2. Anticancer potential

The cytotoxic assay was determined in vitro towards breast carcinoma cell line (MCF-7), liver cancer cell line (HepG-2) and lung cancer cell lung (A549) adapting MTT assay using doxorubicin as a standard [72].

3.3. Docking study

The crystal structure of the epidermal growth factor receptor (EGFR) (PDB: 1M17) was downloaded from Protein Data Bank. A docking study was carried out by CB-DOCK2 applying the reported procedure [73]. The profiles of binding and visualization were carried out for the best-docked complexes using Discovery Studio software.

3.4. ADME study and drug-likeness

Molsoft and Molinspiration were utilized to predict the Lipinski rule for five and drug-likeness.

3.5. QSAR model

It should be noted that such combinations may undermine the model's linear approximation assumption. The QSAR descriptors for all molecules were calculated using MOE molecular descriptors and the multiple linear regression analysis was studied using IBM SPSS statistic 26. The predictor factors utilized in this study are summarized and defined in Table 5.

Table 5: Some symbols for the QSAR descriptors and their definition

Symbol	Definition
ELUMO	energy of the lowest unoccupied molecular orbital
EHOMO	energy of the highest occupied molecular orbital
μ	dipole moment
logP(o/w)	log of the octanol/water partition

	coefficientc
Mr	molecular weight
Esolv	Energy of solvation power
acc	Number of acceptor groups
don	Number of donating groups
AM1_IP	Ionization potential

4. Conclusion

Compound 2f showed the best fit within EGFR active regions, and because of its potent anti-cancer activity against A549 and HepG2 cell lines, it may be pursued as a lead potential anti-cancer candidate. Further optimisation and development are required to evaluate the possibility of introducing this compound in cancer management.

5. Conflict of interest:

No conflict of interest to declare

6. Acknowledgment

The authors extend their appreciation to the Deanship of Scientific Research at Jouf University for funding this work through research grant No (DSR-2021-03-0117)

7. Funding:

The Deanship of Scientific Research funded this manuscript at Jouf University for funding this work through research grant No (DSR-2021-03-0117)

8. References

- Maguire, A.R.; Papot, S.; Ford, A.; Touhey, S.; O'Connor, R.; Clynes, M. Enantioselective synthesis of sulindac. *Synlett* **2001**, 2001, 0041-0044.
- Qiu, G.; Wu, J. Generation of indene derivatives by tandem reactions. *Synlett* **2014**, 25, 2703-2713.
- Clegg, N.J.; Paruthiyil, S.; Leitman, D.C.; Scanlan, T.S. Differential response of estrogen receptor subtypes to 1, 3-diarylindene and 2, 3-diarylindene ligands. *Journal of medicinal chemistry* **2005**, 48, 5989-6003.
- Jeyachandran, M.; Ramesh, P. Synthesis, antimicrobial, and anticoagulant activities of 2-(arylsulfonyl) indane-1, 3-diones. *Organic Chemistry International* **2011**, 2011.
- MIOSRA, R.; Pandey, R.C.; Hilton, B.D.; ROLLER, P.P.; SILVERTON, J.V. Structure of fredericamycin a, an antitumor antibiotic of a novel skeletal type; spectroscopic and mass spectral characterization. *The Journal of Antibiotics* **1987**, 40, 786-802.
- Wang, Y.; Liu, H.-X.; Chen, Y.-C.; Sun, Z.-H.; Li, H.-H.; Li, S.-N.; Yan, M.-L.; Zhang, W.-M. Two new metabolites from the endophytic fungus

- alternaria sp. A744 derived from morinda officinalis. *Molecules* **2017**, *22*, 765.
- Pandey, R.C.; TOUSSAINT, M.W.; STROSHANE, R.M.; KALITA, C.C.; ASZALOS, A.A.; GARRETSON, A.L.; WEI, T.T.; BYRNE, K.M.; WHITE, R.J. Fredericamycin a, a new antitumor antibiotic i. Production, isolation and physicochemical properties. *The Journal of Antibiotics* **1981**, *34*, 1389-1401.
 - Warnick-Pickle, D.J.; BYRNE, K.M.; PANDEY, R.C.; WHITE, R.J. Fredericamycin a, a new antitumor antibiotic ii. Biological properties. *The Journal of Antibiotics* **1981**, *34*, 1402-1407.
 - de Souza, A.P.; Costa, M.C.; de Aguiar, A.R.; Bressan, G.C.; de Almeida Lima, G.D.; Lima, W.P.; Borsodi, M.P.; Bergmann, B.R.; Ferreira, M.M.; Teixeira, R.R. Leishmanicidal and cytotoxic activities and 4d-qsar of 2-arylidene indan-1, 3-diones. *Archiv der Pharmazie* **2021**, *354*, 2100081.
 - Tang, M.-L.; Zhong, C.; Liu, Z.-Y.; Peng, P.; Liu, X.-H.; Sun, X. Discovery of novel sesquiterpene indanone analogues as potent anti-inflammatory agents. *European journal of medicinal chemistry* **2016**, *113*, 63-74.
 - Patel, A.; Giles, D.; Basavarajaswamy, G.; Sreedhar, C.; Patel, A. Synthesis, pharmacological evaluation and molecular docking studies of indanone derivatives. *Medicinal Chemistry Research* **2012**, *21*, 4403-4411.
 - Xiao, S.; Zhang, W.; Chen, H.; Fang, B.; Qiu, Y.; Chen, X.; Chen, L.; Shu, S.; Zhang, Y.; Zhao, Y. Design, synthesis, and structure-activity relationships of 2-benzylidene-1-indanone derivatives as anti-inflammatory agents for treatment of acute lung injury. *Drug Design, Development and Therapy* **2018**, *12*, 887.
 - Patil, S.A.; Patil, R.; Patil, S.A. Recent developments in biological activities of indanones. *European journal of medicinal chemistry* **2017**, *138*, 182-198.
 - Patel, V.M.; Bhatt, N.D.; Bhatt, P.V.; Joshi, H.D. Novel derivatives of 5, 6-dimethoxy-1-indanone coupled with substituted pyridine as potential antimicrobial agents. *Arabian Journal of Chemistry* **2018**, *11*, 137-142.
 - Venkatesh, N.; Sundergoud, S.; Swamy, M.K.; Veerasomaiah, P. Microwave-assisted synthesis and antimicrobial activity of novel pyrazole-indanone hybrid analogs. *Russian Journal of Organic Chemistry* **2020**, *56*, 1635-1639.
 - Adole, V.A.; More, R.A.; Jagdale, B.S.; Pawar, T.B.; Chobe, S.S.; Shinde, R.A.; Dhonnar, S.L.; Koli, P.B.; Patil, A.V.; Bukane, A.R. Microwave prompted solvent-free synthesis of new series of heterocyclic tagged 7-arylidene indanone hybrids and their computational, antifungal, antioxidant, and cytotoxicity study. *Bioorganic Chemistry* **2021**, *115*, 105259.
 - Nel, M.S.; Petzer, A.; Petzer, J.P.; Legoabe, L.J. 2-heteroarylidene-1-indanone derivatives as inhibitors of monoamine oxidase. *Bioorganic chemistry* **2016**, *69*, 20-28.
 - Aucamp, E. An investigation of indanone derivatives as inhibitors of monoamine oxidase. North-West University (South Africa), Potchefstroom Campus, 2018.
 - Glisoni, R.J.; Chiappetta, D.A.; Moglioni, A.G.; Sosnik, A. Novel 1-indanone thiosemicarbazone antiviral candidates: Aqueous solubilization and physical stabilization by means of cyclodextrins. *Pharmaceutical research* **2012**, *29*, 739-755.
 - Glisoni, R.J.; Cuestas, M.L.; Mathet, V.L.; Oubiña, J.R.; Moglioni, A.G.; Sosnik, A. Antiviral activity against the hepatitis c virus (hcv) of 1-indanone thiosemicarbazones and their inclusion complexes with hydroxypropyl- β -cyclodextrin. *European journal of pharmaceutical sciences* **2012**, *47*, 596-603.
 - Santacruz, M.C.S.; Fabiani, M.; Castro, E.F.; Cavallaro, L.V.; Finkielstein, L.M. Synthesis, antiviral evaluation and molecular docking studies of n4-aryl substituted/unsubstituted thiosemicarbazones derived from 1-indanones as potent anti-bovine viral diarrhea virus agents. *Bioorganic & Medicinal Chemistry* **2017**, *25*, 4055-4063.
 - Kurkin, A.V.; Curreli, F.; Iusupov, I.R.; Spiridonov, E.A.; Ahmed, S.; Markov, P.O.; Manasova, E.V.; Altieri, A.; Debnath, A.K. Design, synthesis, and antiviral activity of the thiazole positional isomers of a potent hiv-1 entry inhibitor nbd-14270. *ChemMedChem* **2022**, *17*, e202200344.
 - Singh, A.; Fatima, K.; Srivastava, A.; Khwaja, S.; Priya, D.; Singh, A.; Mahajan, G.; Alam, S.; Saxena, A.K.; Mondhe, D. Anticancer activity of gallic acid template-based benzylidene indanone derivative as microtubule destabilizer. Wiley Online Library: 2016; Vol. 88, pp 625-634.
 - Abolhasani, H.; Zarghi, A.; Movahhed, T.K.; Abolhasani, A.; Daraei, B.; Dastmalchi, S. Design, synthesis and biological evaluation of novel indanone containing spiroisoxazoline derivatives with selective cox-2 inhibition as anticancer agents. *Bioorganic & Medicinal Chemistry* **2021**, *32*, 115960.
 - Saxena, H.O.; Faridi, U.; Srivastava, S.; Kumar, J.; Darokar, M.; Luqman, S.; Chanotiya, C.; Krishna, V.; Negi, A.S.; Khanuja, S. Gallic acid-based indanone derivatives as anticancer agents. *Bioorganic & Medicinal Chemistry Letters* **2008**, *18*, 3914-3918.

26. Barreca, M.; Spanò, V.; Raimondi, M.V.; Tarantelli, C.; Spriano, F.; Berton, F.; Barraja, P.; Montalbano, A. Recurrence of the oxazole motif in tubulin colchicine site inhibitors with anti-tumor activity. *European Journal of Medicinal Chemistry Reports* **2021**, *1*, 100004.
27. El-Sherief, H.A.; Youssif, B.G.; Bukhari, S.N.A.; Abdel-Aziz, M.; Abdel-Rahman, H.M. Novel 1, 2, 4-triazole derivatives as potential anticancer agents: Design, synthesis, molecular docking and mechanistic studies. *Bioorganic chemistry* **2018**, *76*, 314-325.
28. Barreca, M.; Spanò, V.; Rocca, R.; Bivacqua, R.; Abel, A.-C.; Maruca, A.; Montalbano, A.; Raimondi, M.V.; Tarantelli, C.; Gaudio, E. Development of [1, 2] oxazoloisindoles tubulin polymerization inhibitors: Further chemical modifications and potential therapeutic effects against lymphomas. *European Journal of Medicinal Chemistry* **2022**, *243*, 114744.
29. Zeid, I.F.; Said, M.M.; Darwish, S.A.; Soliman, F.M. Chemistry of phosphorus ylides. Part 38: Synthesis and anticancer activity of cyclobutane, oxaphosphetane, oxaphosphinine, azaphosphetidene, and pyridazine derivatives. *Monatshefte für Chemie-Chemical Monthly* **2014**, *145*, 639-650.
30. Shubakara, K.; Umesha, K.; Srikantamurthy, N.; Chethan, J. Antioxidant and DNA damage inhibition activities of 4-aryl-n-(4-aryl-thiazol-2-yl)-5, 6-dihydro-4h-1, 3, 4-oxadiazine-2-carboxamides. *Journal of Chemical Sciences* **2014**, *126*, 1913-1921.
31. Pasha, M.A.; Mondal, S.; Panigrahi, N. Review of synthetic strategies in the development of oxadiazine scaffolds. *Mediterranean Journal of Chemistry* **2019**, *8*, 338-364.
32. Akbar, S.; Das, S.; Iqbal, A.; Ahmed, B. Synthesis, biological evaluation and molecular dynamics studies of oxadiazine derivatives as potential anti-hepatotoxic agents. *Journal of Biomolecular Structure and Dynamics* **2021**, 1-18.
33. Zhang, J.; Hao, W.; Zhorov, B.S.; Dong, K.; Jiang, D. Discovery of a novel series of tricyclic oxadiazine 4a-methyl esters based on indoxacarb as potential sodium channel blocker/modulator insecticides. *Journal of agricultural and food chemistry* **2019**, *67*, 7793-7809.
34. Wing, K.D.; Sacher, M.; Kagaya, Y.; Tsurubuchi, Y.; Mulderig, L.; Connair, M.; Schnee, M. Bioactivation and mode of action of the oxadiazine indoxacarb in insects. *Crop Protection* **2000**, *19*, 537-545.
35. Bakavoli, M.; Rahimizadeh, M.; Shiri, A.; Eshghi, H.; Vaziri-Mehr, S.; Pordeli, P.; Nikpour, M. Synthesis and evaluation of antibacterial activity of new derivatives of pyrimido [4, 5-e][1, 3, 4] oxadiazine. **2011**.
36. Gurunanjappa, P.; Kariyappa, A.K. An easy procedure for synthesis of 1, 3, 4-oxadiazines: A potential antimicrobial agents. *Asian Journal of Chemistry* **2017**, *29*, 1687-1689.
37. Pérez, S.; Lasheras, B.; Oset, C.; Monge, A. Synthesis of new indoyl-1, 3, 4-oxadiazole and oxadiazine derivatives. Potential monoamine oxidase inhibitor activity. *Journal of heterocyclic chemistry* **1997**, *34*, 1527-1533.
38. Bakavoli, M.; Rahimizadeh, M.; Shiri, A.; Akbarzadeh, M.; Mousavi, S.-H.; Atapour-Mashhad, H.; Tayarani-Najaran, Z. Synthesis and anticancer evaluation of new derivatives of 3-phenyl-1, 5-dimethyl-1h-[1, 2, 4] triazolo [4', 3': 1, 2] pyrimido [4, 5-e][1, 3, 4] oxadiazine. *Journal of chemical Research* **2010**, *34*, 403-406.
39. Voráčová, K.; Hájek, J.; Mareš, J.; Urajová, P.; Kuzma, M.; Cheel, J.; Villunger, A.; Kapuscik, A.; Bally, M.; Novák, P. The cyanobacterial metabolite nocuolin a is a natural oxadiazine that triggers apoptosis in human cancer cells. *PLoS One* **2017**, *12*, e0172850.
40. Shetnev, A.A.; Zubkov, F.I. The latest advances in chemistry of 1, 2, 4-oxadiazines (microreview). *Chemistry of Heterocyclic Compounds* **2017**, *53*, 495-497.
41. Mohareb, R.M.; Ibrahim, R.A.; Moustafa, H.E. Hydrazide-hydrazone in the synthesis of 1, 3, 4-oxadiazine, 1, 2, 4-triazine and pyrazole derivatives with antitumor activities. *The Open Organic Chemistry Journal* **2010**, *4*.
42. Ahmed, K. Prasad, nvsd evaluation of indoxacarb 15% sc against fruit borers in chillies. Pestology: 2011.
43. Ye, Z.; Xia, S.; Shao, X.; Cheng, J.; Xu, X.; Xu, Z.; Li, Z.; Qian, X. Design, synthesis, crystal structure analysis, and insecticidal evaluation of phenylazoneonicotinoids. *Journal of agricultural and food chemistry* **2011**, *59*, 10615-10623.
44. Lapied, B.; Grolleau, F.; Sattelle, D.B. Indoxacarb, an oxadiazine insecticide, blocks insect neuronal sodium channels. *British journal of pharmacology* **2001**, *132*, 587-595.
45. Alanazi, M.A.; Arafa, W.A.; Althobaiti, I.O.; Altaleb, H.A.; Bakr, R.B.; Elkanzi, N.A. Green design, synthesis, and molecular docking study of novel quinoxaline derivatives with insecticidal potential against aphid craccivora. *ACS omega* **2022**, *7*, 27674-27689.
46. Bakr, R.B.; Elkanzi, N.A. Novel 1, 2-thiazine-pyridine hybrid: Design, synthesis, antioxidant activity and molecular docking study. *Letters in Drug Design & Discovery* **2022**, *19*, 675-690.
47. Abdelgawad, M.A.; Elkanzi, N.A.; Musa, A.; Ghoneim, M.M.; Ahmad, W.; Elmowafy, M.; Ali,

- A.M.A.; Abdelazeem, A.H.; Bukhari, S.N.; El-Sherbiny, M. Optimization of pyrazolo [1, 5-a] pyrimidine based compounds with pyridine scaffold: Synthesis, biological evaluation and molecular modeling study. *Arabian Journal of Chemistry* **2022**, 104015.
48. Elkanzi, N.A.; Hrichi, H.; Alolayan, R.A.; Derafa, W.; Zahou, F.M.; Bakr, R.B. Synthesis of chalcones derivatives and their biological activities: A review. *ACS omega* **2022**, 7, 27769-27786.
49. Abdelgawad, M.A.; Al-Sanea, M.M.; Musa, A.; Elmowafy, M.; El-Damasy, A.K.; Azouz, A.A.; Ghoneim, M.M.; Bakr, R.B. Docking study, synthesis, and anti-inflammatory potential of some new pyridopyrimidine-derived compounds. *Journal of Inflammation Research* **2022**, 15, 451.
50. Abdelgawad, M.A.; Elkanzi, N.A.; Nayl, A.; Musa, A.; Alotaibi, N.H.; Arafa, W.; Gomha, S.M.; Bakr, R.B. Targeting tumor cells with pyrazolo [3, 4-d] pyrimidine scaffold: A literature review on synthetic approaches, structure activity relationship, structural and target-based mechanisms. *Arabian Journal of Chemistry* **2022**, 103781.
51. Abdelgawad, M.A.; Musa, A.; Almalki, A.H.; Alzarea, S.I.; Mostafa, E.M.; Hegazy, M.M.; Mostafa-Hedeab, G.; Ghoneim, M.M.; Parambi, D.G.; Bakr, R.B. Novel phenolic compounds as potential dual egfr and cox-2 inhibitors: Design, semisynthesis, in vitro biological evaluation and in silico insights. *Drug design, development and therapy* **2021**, 15, 2325.
52. AL-Shammri, K.N.; Elkanzi, N.A.; Arafa, W.A.; Althobaiti, I.O.; Bakr, R.B.; Moustafa, S.M.N. Novel indan-1, 3-dione derivatives: Design, green synthesis, effect against tomato damping-off disease caused by fusarium oxysporum and in silico molecular docking study. *Arabian Journal of Chemistry* **2022**, 15, 103731.
53. Bakr, R.B.; Mehany, A. (3, 5-dimethylpyrazol-1-yl)-[4-(1-phenyl-1h-pyrazolo [3, 4-d] pyrimidin-4-ylamino) phenyl] methanone. *Molbank* **2016**, 2016, M915.
54. El Azab, I.H.; El-Sheshtawy, H.S.; Bakr, R.B.; Elkanzi, N.A. New 1, 2, 3-triazole-containing hybrids as antitumor candidates: Design, click reaction synthesis, dft calculations, and molecular docking study. *Molecules* **2021**, 26, 708.
55. De Clercq, E.; Descamps, J.; Verhelst, G.; Walker, R.; Jones, A.; Torrence, P.; Shugar, D. Comparative efficacy of antiherpes drugs against different strains of herpes simplex virus. *Journal of Infectious Diseases* **1980**, 141, 563-574.
56. Estrada, E.; Uriarte, E.; Montero, A.; Teixeira, M.; Santana, L.; De Clercq, E. A novel approach for the virtual screening and rational design of anticancer compounds. *Journal of medicinal chemistry* **2000**, 43, 1975-1985.
57. Xiao, Z.; Xiao, Y.-D.; Feng, J.; Golbraikh, A.; Tropsha, A.; Lee, K.-H. Antitumor agents. 213. Modeling of epipodophyllotoxin derivatives using variable selection k nearest neighbor qsar method. *Journal of medicinal chemistry* **2002**, 45, 2294-2309.
58. McKinney, J.; Darden, T.; Lyerly, M.A.; Pedersen, L. Pcb and related compound binding to the ah receptor (s) theoretical model based on molecular parameters and molecular mechanics. *Quantitative Structure-Activity Relationships* **1985**, 4, 166-172.
59. Waller, C.L.; McKinney, J.D. Comparative molecular field analysis of polyhalogenated dibenzo-p-dioxins, dibenzofurans, and biphenyls. *Journal of medicinal chemistry* **1992**, 35, 3660-3666.
60. Tuppurainen, K.; Ruuskanen, J. Electronic eigenvalue (eeva): A new qsar/qspr descriptor for electronic substituent effects based on molecular orbital energies. A qsar approach to the ah receptor binding affinity of polychlorinated biphenyls (pcbs), dibenzo-p-dioxins (pcdds) and dibenzofurans (pcdfs). *Chemosphere* **2000**, 41, 843-848.
61. Blackadar, C.B. Historical review of the causes of cancer. *World journal of clinical oncology* **2016**, 7, 54.
62. Mahvi, D.A.; Liu, R.; Grinstaff, M.W.; Colson, Y.L.; Raut, C.P. Local cancer recurrence: The realities, challenges, and opportunities for new therapies. *CA: a cancer journal for clinicians* **2018**, 68, 488-505.
63. Clapp, R.W.; Jacobs, M.M.; Loechler, E.L. Environmental and occupational causes of cancer: New evidence 2005-2007. *Reviews on environmental health* **2008**, 23, 1-38.
64. Kausar, S.; Falcao, A.O. An automated framework for qsar model building. *Journal of cheminformatics* **2018**, 10, 1-23.
65. Rogers, D.; Hopfinger, A.J. Application of genetic function approximation to quantitative structure-activity relationships and quantitative structure-property relationships. *Journal of Chemical Information and Computer Sciences* **1994**, 34, 854-866.
66. B Bakr, R.; BM Mehany, A.; RA Abdellatif, K. Synthesis, egfr inhibition and anti-cancer activity of new 3, 6-dimethyl-1-phenyl-4-(substituted-methoxy) pyrazolo [3, 4-d] pyrimidine derivatives. *Anti-Cancer Agents in Medicinal Chemistry (Formerly Current Medicinal Chemistry-Anti-Cancer Agents)* **2017**, 17, 1389-1400.

67. Abdelgawad, M.A.; Bakr, R.B.; Alkhoja, O.A.; Mohamed, W.R. Design, synthesis and antitumor activity of novel pyrazolo [3, 4-d] pyrimidine derivatives as egfr-tk inhibitors. *Bioorganic chemistry* **2016**, *66*, 88-96.
68. Barr, S.; Thomson, S.; Buck, E.; Russo, S.; Petti, F.; Sujka-Kwok, I.; Eyzaguirre, A.; Rosenfeld-Franklin, M.; Gibson, N.W.; Miglarese, M. Bypassing cellular egf receptor dependence through epithelial-to-mesenchymal-like transitions. *Clinical & experimental metastasis* **2008**, *25*, 685-693.
69. Berasain, C.; Latasa, M.U.; Urtasun, R.; Goñi, S.; Elizalde, M.; Garcia-Irigoyen, O.; Azcona, M.; Prieto, J.; Ávila, M.A. Epidermal growth factor receptor (egfr) crosstalks in liver cancer. *Cancers* **2011**, *3*, 2444-2461.
70. Lotfy, G.; El Sayed, H.; Said, M.M.; Aziz, Y.M.A.; Al-Dhfyan, A.; Al-Majid, A.M.; Barakat, A. Regio- and stereoselective synthesis of new spirooxindoles via 1, 3-dipolar cycloaddition reaction: Anticancer and molecular docking studies. *Journal of Photochemistry and Photobiology B: Biology* **2018**, *180*, 98-108.
71. Alosaimy, A.M.; Abouzied, A.S.; Alsaedi, A.M.; Alafnan, A.; Alamri, A.; Alamri, M.A.; Break, M.K.B.; Sabour, R.; Farghaly, T.A. Discovery of novel indene-based hybrids as breast cancer inhibitors targeting hsp90: Synthesis, bio-evaluation and molecular docking study. *Arabian Journal of Chemistry* **2023**, 104569.
72. El Azab, I.H.; Bakr, R.B.; Elkanzi, N.A. Facile one-pot multicomponent synthesis of pyrazolo-thiazole substituted pyridines with potential anti-proliferative activity: Synthesis, in vitro and in silico studies. *Molecules* **2021**, *26*, 3103.
73. Ghoneim, M.M.; Al-Serwi, R.H.; El-Sherbiny, M.; El-ghaly, E.-s.M.; Hamad, A.E.; Abdelgawad, M.A.; Ragab, E.A.; Bukhari, S.I.; Bukhari, K.; Elokely, K. Proposed mechanism for emodin as agent for methicillin resistant staphylococcus aureus: In vitro testing and in silico study. *Current Issues in Molecular Biology* **2022**, *44*, 4490-4499.